

# Highly efficient fiber-to-chip evanescent coupling based on subwavelength-diameter optical fibers

Xiaowei Shen (沈晓伟), Xinwan Li (李新碗)\*, Linjie Zhou (周林杰), Zehua Hong (洪泽华), Xiaocao Yu (余小草), Ying Zhang (张英), and Jianping Chen (陈建平)

State Key Laboratory of Advanced Optical Communication Systems and Networks, Department of Electronic Engineering, Shanghai Jiao Tong University, Shanghai 200030, China

\*Corresponding author: [lixinwan@sjtu.edu.cn](mailto:lixinwan@sjtu.edu.cn)

Received October 27, 2010; accepted December 17, 2010; posted online April 18, 2011

A novel, compact, and highly efficient fiber-to-chip evanescent coupling structure is proposed based on a subwavelength-diameter fiber. The coupling structure is characterized by a large misalignment tolerance and easy fabrication. The dependence of coupling efficiency on various parameters is calculated and analyzed. The simulation results show that a coupling efficiency as high as 95% can be obtained within a coupling length of  $<4 \mu\text{m}$ .

OCIS codes: 060.2340, 130.3120.

doi: 10.3788/COL201109.050604.

Due to its versatility in terms of functions and compatibility with complementary metal-oxide-semiconductor (CMOS) technologies, silicon photonics are expected to play an important role in inter-/intra-chip interconnection and optical fiber communication<sup>[1]</sup>. However, the high refractive index contrast in silicon waveguides (Si-WGs) and the resulting mode mismatch with single-mode fibers (SMFs) make the realization of efficient coupling between Si-WGs and SMFs a challenging task. Adiabatic tapers, both normal and inverted tapers, and grating couplers are the two most widely used highly efficient coupling structures<sup>[2]</sup>. Inverted tapers rely on mode expansion to butt-couple with optical fibers, and they usually require a long taper length ( $>40 \mu\text{m}$ ). Moreover, the alignment is usually significant due to its tiny taper tip ( $\sim 50 \text{ nm}$ )<sup>[3,4]</sup>. Couplers consisting of high-order multi-stages of rib tapers are another class of adiabatic taper structures in which light from the fiber is coupled into a mode-matched rib taper and is gradually “squeezed” into the beneath silicon waveguide. Such couplers release the alignment requirement. However, the complexity in their structures makes the fabrication process more difficult, and they usually require a relatively long taper length ( $>100 \mu\text{m}$ )<sup>[5,6]</sup>. Coupling through grating couplers can also relax the stringent alignment requirement, however, their coupling efficiency is relatively low and essentially wavelength dependent, thereby limiting their widespread use. Although a high coupling efficiency can be achieved by designing complex grating structures, this also increases fabrication difficulty. Moreover, a long grating coupler length ( $>100 \mu\text{m}$ ) is also inevitable<sup>[7–9]</sup>.

Recently, advancements on subwavelength-diameter fibers (SDFs) have attracted considerable research attentions. As SDFs are drawn from SMFs, the adiabatic decrease in fiber diameter thus forms a natural low-loss transformer for the light to couple from SMF to SDF<sup>[10,11]</sup>. The SDF has a long evanescent tail outside the cladding, making the realization of a highly efficient evanescent coupling to a Si-WG within a quite short coupling length possible. In this letter, we propose a SDF to Si-WG coupling structure in which the SDF is side-attached to a suspended Si-WG through Casimir

force<sup>[12]</sup>. We analyze the influences of the geometrical parameters of the SDF and Si-WG on the coupling efficiency using three-dimensional finite element method (FEM) simulations.

Figure 1 shows our proposed SDF to Si-WG coupling structure. The SDF ( $n_{\text{fiber}}=1.46$  at  $1550 \text{ nm}$ ) drawn from a SMF using hydrogen heating is positioned close to a suspended Si-WG ( $n_{\text{si}}=3.48$  at  $1550 \text{ nm}$ ). As a result of the strong Casimir force between them, they eventually stick together. We choose typical Si-WG dimensions of  $250\text{-nm}$  height and  $500\text{-nm}$  width for our numerical simulations. Note that the suspended Si-WG can be fabricated by removing the underlying  $\text{SiO}_2$  using HF chemical etching. In the model, an optical light with  $1550\text{-nm}$  wavelength is excited into the input end of the SDF, and the output power from the Si-WG is collected. The coupling efficiency is then obtained as  $\eta = P_{\text{out}}/P_{\text{in}}$ , where  $P_{\text{in}}$  and  $P_{\text{out}}$  are the input and output optical powers, respectively.

Coupling light directly from the SDF to Si-WG is difficult<sup>[13]</sup>. As shown in Figs. 2(a) and (b), on one hand, the large effective refractive index difference between the SDF and Si-WG results in a high-order mode ( $n_{\text{eff}}=1.106$ ) excitation in Si-WG, causing coupling loss. On the other hand, the large Si-WG facet size also causes scattering loss. To address these problems, we design a taper structure in which the Si-WG is tapered down along one side to a  $50\text{-nm}$ -wide tip, whereas the other side

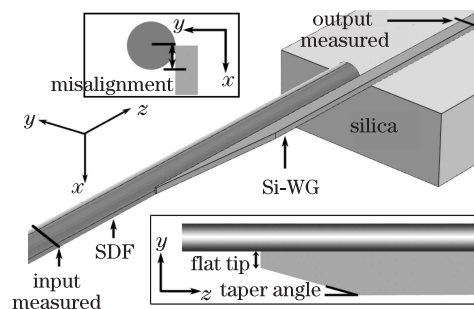


Fig. 1. SDF to Si-WG coupling structure using a suspended taper structure.

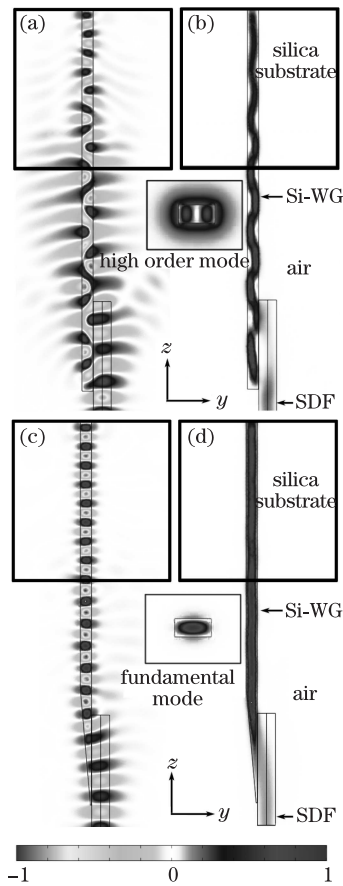


Fig. 2. (a) Transverse electric field and (b) optical power profile in a non-taper structure; (c) transverse electric field and (d) optical power profile in a taper structure.

remains flat, favoring the SDF attachment. Figures 2(c) and (d) show the transverse electric (TE) field ( $E_x$ ) and optical power flow patterns for the proposed taper structure, assuming that the input light is TE polarized. The geometrical parameters are as follows: SDF diameter of 700 nm, taper angle of  $5^\circ$ , taper tip width of 50 nm, coupling length of  $5 \mu\text{m}$ , and no misalignment. Due to the taper structure, energy can be transferred from the SDF to the Si-WG smoothly without exciting high-order modes and inducing excess scattering loss. The coupling efficiency is as high as 92%, and its transmission spectrum is shown in Fig. 3. This shows that the coupling efficiency is relatively flat over a wide wavelength range.

The SDF mode profile, Si-WG taper shape, and their relative positions have critical effects on the coupling efficiency. In the following analysis, we mainly focus on the SDF diameter, taper angle, taper tip width, coupling length, and misalignment as we examine their influences on the coupling efficiency using FEM simulations. We vary one parameter and study its effect on the coupling efficiency, and the other parameters are chosen as in Figs. 2(c) and (d).

The fiber diameter affects the mode confinement factor and effective refractive index of the SDFs. The confinement factor reflects the capability to confine optical energy in the fiber core. The smaller the confinement factor, the larger the evanescent field, which favors the coupling between the SDF and the Si-WG. However, a low optical confinement also increases the propagation

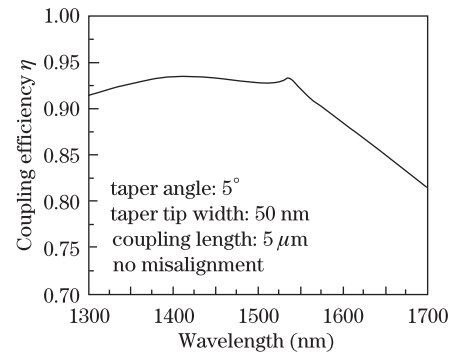


Fig. 3. Coupling efficiency versus wavelength in a taper structure.

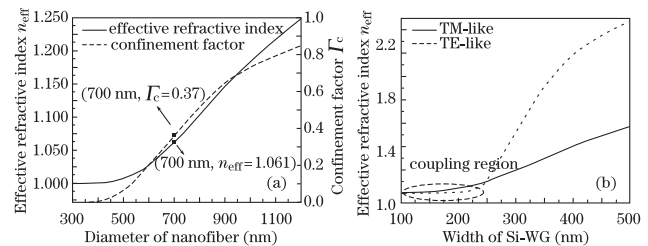


Fig. 4. (a) SDF mode analysis; (b) Si-WG mode analysis.

loss and makes the SDF very sensitive to small variations on the fiber surface. The matched effective refractive indices of the SDF and the Si-WG lead to identical propagation constants, which also favor optical coupling due to phase matching. Therefore, we need to find an optimum SDF diameter to obtain the maximum coupling efficiency.

Figure 4(a) shows the dependence of the effective refractive index and the confinement factor on the SDF diameter. Figure 4(b) shows the dependence of the effective refractive index on the Si-WG width for quasi-TE and quasi-TM modes. To obtain matched effective refractive indices, the SDF diameter should be  $<800 \text{ nm}$ . The diameter should also be  $>400 \text{ nm}$  to avoid a small confinement factor. The simulation shows that the highest coupling efficiency occurs at an SDF diameter of 700 nm.

Figure 5 shows the dependence of coupling efficiency on the taper angle for various SDF diameters. As expected, a small taper angle can prevent a higher-order mode excitation in Si-WG as well as provide enough spatial overlap for the SDF and the Si-WG optical modes. Essentially, the smaller the taper angle ( $<5^\circ$ ), the higher the coupling efficiency. The coupling efficiency for a  $3.5^\circ$  taper almost reaches 95%, but this sacrifices a longer coupling length of  $7.5 \mu\text{m}$ , thereby making it less compact. For a  $5^\circ$  taper angle, the coupling efficiency reaches 92%. When the taper angle exceeds about  $10^\circ$ , part of the optical energy begins to couple into the higher-order modes of the Si-WG, therefore lowering the coupling efficiency. When the taper angle exceeds about  $30^\circ$ , the percentage of optical energy coupled into the Si-WG remains at a relatively low level regardless of how sharp the taper tip is. Further study reveals that most of the optical energy is either coupled to the high-order modes or is scattered by the taper.

An infinite sharp taper tip is unrealistic to fabricate, and so the influence of the Si-WG taper tip width should

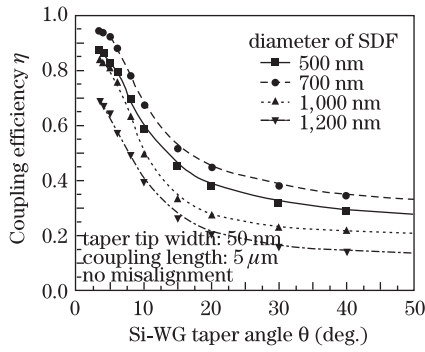


Fig. 5. Coupling efficiency changes as a function of Si-WG taper angle.

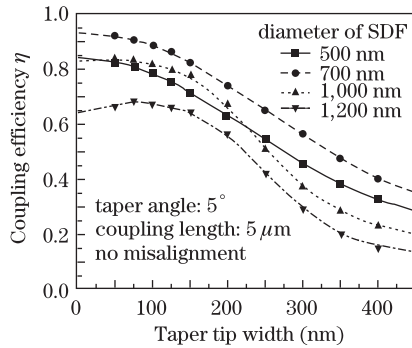


Fig. 6. Coupling efficiency changes as a function of taper tip width.

be taken into account. The flat tip acts as a perturbation to the SDF refractive index, which in principle can cause scattering loss. Encouragingly, the simulation result in Fig. 6 shows that a small flat tip has very little effect as long as the tip width is  $<100$  nm.

SDFs with a diameter  $<1,000$  nm have an expanded mode pattern, which can easily be scattered by the Si-WG taper tip. Wider Si-WG taper tips scatter the evanescent field more, and so the coupling efficiency is lowered with the taper tip width. When the tip width exceeds a certain value, which is 200 nm in our case, the effective refractive index of the Si-WG taper mismatches that of the SDF according to Fig. 4(b), and the high-order decaying modes of the Si-WG are excited, causing a rapid decrease in the coupling efficiency. For SDFs with a diameter  $>1,000$  nm in which the confinement factor is relatively large ( $>0.85$ ), and most optical energy is localized in the fiber, taper tip-induced scattering is less significant. The coupling efficiency increases first and then decreases rapidly with the taper tip width, and the optimum coupling occurs at the tip width of around 70 nm when its effective refractive index is matched with that of the Si-WG.

As mentioned above, one of the shortcomings of conventional taper or grating coupler structures is their relatively long coupling length compared with the submicrometer cross-sectional dimension of Si-WGs. Our proposed coupling structure, however, has a relatively short coupling length due to the strong coupling between the SDF and the Si-WG.

Figure 7 shows the dependence of coupling efficiency on the coupling length for various SDF diameters. When the SDF diameter is below 500 nm, the optical energy can instantly be transferred from the SDF to the Si-WG.

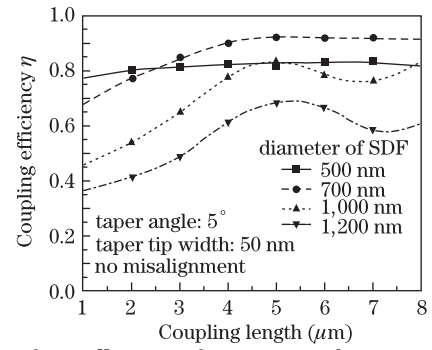


Fig. 7. Coupling efficiency changes as a function of coupling length.

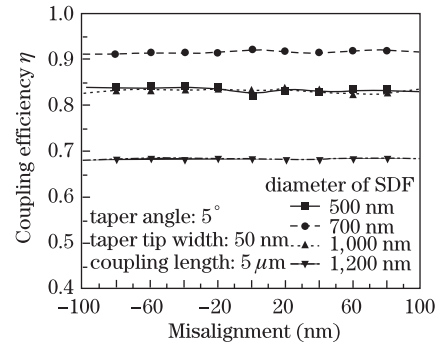


Fig. 8. Coupling efficiency changes as a function of misalignment between Si-WG and SDF.

When the SDF diameter is around 700 nm, a coupling efficiency of  $>90\%$  can be obtained within a coupling length of  $4 \mu\text{m}$ . Further, no energy circulating transfer occurs due to the large difference in effective refractive indices caused by the taper structure. The stable coupling favors the easy assembling in pigtail package applications. However, when the SDF diameter is above 1,000 nm, the maximum coupling efficiency occurs at a relatively long coupling length of  $>5 \mu\text{m}$ , and the coupling efficiency also oscillates with the coupling length due to the interference of the fundamental and high-order Si-WG modes.

One of the factors causing a dramatic loss in butt-coupling is the misalignment between the fiber tip ( $\sim 50$  nm) and the Si-WG. Therefore, examining the influence of misalignment on the coupling efficiency is important. Considering the coupling structure shown in Fig. 1 wherein the SDF is misaligned to the Si-WG, which is due to the strong Casimir force, the SDF and the Si-WG taper can be auto-aligned as long as they are close to each other. Figure 8 shows the dependence of coupling efficiency on the misalignment for various SDF diameters. The simulation results show that the misalignment has a negligible effect on the coupling efficiency, which is probably due to the large evanescent field associated with the SDF compared with the small misalignment value.

In this letter, we use a suspended Si-WG to couple with a SDF because the SDF can easily attach to the Si-WG sidewall in order to obtain a high coupling efficiency. Figure 9(a) shows a non-suspended taper structure wherein the Si-WG taper is supported by a silica-on-silicon substrate beneath. Light can easily leak into the silicon substrate before coupled into the Si-WG. As shown in Fig. 9(b), the coupling efficiency of a non-suspended

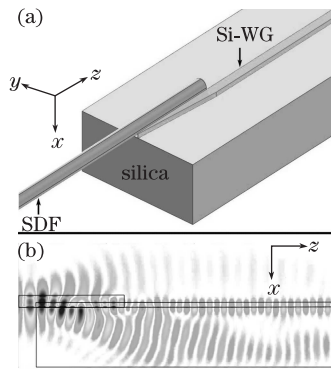


Fig. 9. (a) SDF to Si-WG coupling structure using a non-suspended taper structure; (b) transverse electric field.

taper structure deteriorates substantially ( $<40\%$ ). Therefore, etching off the silica layer beneath the taper to avoid excess leakage is necessary.

Although we only use simulations to analyze the coupling performance, the coupler structure is quite feasible in practice. Firstly, due to the strong Casimir force existing between the SDF and the Si-WG, the former can tightly stick to the suspended Si-WG. Essentially, due to the large evanescent field associated with the SDF, even non-zero separation, which might be attributed to dust or a rugged surface, for example, will not significantly affect the coupling efficiency. For example, keeping other structure parameters unchanged, when the separation increases to 50 nm, the coupling efficiency only decreases by  $<2\%$ , which shows it has a large separation misalignment tolerance. Secondly, the fabrication of such coupling structure is feasible. A 50-nm tip size seems to be non-trivial, however using advanced fabrication tools such as e-beam lithography, for instance, and even a sharper tip (40-nm tip width) has been demonstrated<sup>[14]</sup>. Furthermore, as shown in Fig. 6, there is a large tolerance in taper tip design. Even when the taper tip is as wide as 100 nm, the coupling efficiency is still near 90%, and by reducing the taper angle, a higher coupling efficiency can be obtained. The last concern is the mechanical stability issue. The length of the suspended taper is only 10  $\mu\text{m}$ , and silicon is a very stiff material, so the Si-WG and the proposed coupling structure can possibly maintain good mechanical stability. To favor the pigtail optical package in practice, a low refractive index material Teflon ( $n=1.3$  at 1550 nm) can be applied to cover the whole structure, and then the mechanical stability can be further enhanced<sup>[15]</sup>. In case of Teflon cladding, a coupling efficiency of  $>90\%$  can also be obtained within a coupling length of  $<10 \mu\text{m}$ .

In conclusion, a novel compact SDF to Si-WG coupling structure is proposed, and the dependence of the cou-

pling efficiency on various design parameters is analyzed in this letter. The simulation results show that the coupling efficiency for such compact coupling structure can be as high as 95%. The SDF-based couplers provide a means to guide light efficiently into and out of integrated silicon photonic chips.

This work was supported in part by the National “973” Program of China (No. 2011CB301700), the National Natural Science Foundation of China (Nos. 60877012, 61001074, and 61007039), the Scientific and Technology Commission of Shanghai Municipal Government Project (Nos. 10DJ1400402 and 09JC1408100), the State Key Laboratory Projects (No. GKZD03000X), and the State Key Laboratory of Optoelectronics Project (No. 2010KFB002).

## References

1. W. Bogaerts, R. Baets, P. Dumon, V. Wiaux, S. Beckx, D. Taillaert, B. Luyssaert, J. V. Campenhout, P. Bienstman, and D. V. Thourhout, *J. Lightwave Technol.* **23**, 401 (2005).
2. R. Orobtcchouk, in *Optical Interconnects: the Silicon Approach*, L. Pavesi, G. Guillot, (eds.) (Springer, Berlin 2006) chap. 10.
3. V. R. Almeida, R. R. Panepucci, and M. Lipson, *Opt. Lett.* **28**, 1302 (2003).
4. K. K. Lee, D. R. Lim, D. Pan, C. Hoepfner, W.-Y. Oh, K. Wada, L. C. Kimerling, K. P. Yap, and M. T. Doan, *Opt. Lett.* **30**, 498 (2005).
5. D. Dai, S. He, and H. Tsang, *J. Lightwave Technol.* **24**, 2428 (2006).
6. A. Barkai, A. Liu, D. Kim, R. Cohen, N. Elek, H. Chang, B. H. Malik, R. Gabay, R. Jones, M. Paniccia, and N. Izhaky, *J. Lightwave Technol.* **26**, 3860 (2008).
7. F. Van Laere, G. Roelkens, M. Ayre, J. Schrauwen, D. Taillaert, D. Van Thourhout, T. F. Krauss, and R. Baets, *J. Lightwave Technol.* **25**, 151 (2007).
8. B. Wang, J. Jiang, D. M. Chambers, J. Cai, and G. P. Nordin, *Opt. Lett.* **30**, 845 (2005).
9. G. Roelkens, D. V. Thourhout, and R. Baets, *Opt. Lett.* **32**, 1495 (2007).
10. L. Tong, R. R. Gattass, J. B. Ashcom, S. He, J. Lou, M. Shen, I. Maxwell, and E. Mazur, *Nature* **426**, 816 (2003).
11. J. Fu, X. Yin, N. Li, and L. Tong, *Chin. Opt. Lett.* **6**, 112 (2008).
12. W. H. P. Pernice, M. Li, D. Garcia-Sanchez, and H. X. Tang, *Opt. Express* **18**, 12615 (2010).
13. Z. Zhang, M. Qiu, U. Andersson, and L. Tong, *Chin. Opt. Lett.* **5**, 577 (2007).
14. M. Pu, L. Liu, H. Ou, K. Yvind, and J. M. Hvam, *Opt. Commun.* **283**, 3678 (2010).
15. F. Xu and G. Brambilla, *Opt. Lett.* **32**, 2164 (2007).